

Synchrotron Radiation as the Source of Gamma-Ray Burst Spectra.

Nicole M. Lloyd & Vahé Petrosian

Center for Space Science and Astrophysics, Stanford University, Stanford, California 94305

ABSTRACT

We investigate synchrotron emission models as the source of gamma-ray burst spectra. We show that including the possibility for synchrotron self absorption, a “smooth cutoff” to the electron energy distribution, and an anisotropic distribution for the electron pitch angles produces a whole range of low energy spectral behavior. In addition, we show that the procedure of spectral fitting to GRB data over a finite bandwidth can introduce a spurious correlation between spectral parameters - in particular, the value of the peak of the νF_ν spectrum, E_p , and the low energy photon spectral index α (the lower E_p is, the lower (softer) the fitted value of α will be). From this correlation and knowledge of the E_p distribution, we show how to derive the expected distribution of α . We show that optically thin synchrotron models with an isotropic electron pitch angle distribution can explain the distribution of α below $\alpha = -2/3$. This agreement is achieved if we relax the unrealistic assumption of the presence of a sharp low energy cutoff in the spectrum of accelerated electrons, and allow for a more gradual break. We show that this low energy portion of the electron spectrum can be at most flat. We also show that optically thin synchrotron models with an *anisotropic* electron pitch angle distribution can explain all bursts with $-2/3 \lesssim \alpha \lesssim 0$. The very few bursts with low energy spectral indices that fall above $\alpha = 0$ may be due the presence of a the synchrotron self-absorption frequency entering the lower end of the BATSE window. Our results also predict a particular relationship between α and E_p during the temporal evolution of a GRB. We give examples of spectral evolution in GRBs and discuss how the behavior are consistent with the above models.

1. Introduction

The spectrum of a gamma-ray burst (hereafter, GRB) is a crucial element in understanding the nature of the event. It can provide information about the burst energetics, the local magnetic field, particle distributions and acceleration mechanisms, and the overall expansion of the fireball. Unlike the extreme variation in the light curves, the spectra of GRBs are fairly homogeneous. The photon spectrum of most GRBs in the BATSE spectral energy range can be parameterized by a broken power law with low and high energy photon spectral indices, α and β , and a break energy, E_b (e.g. Band et al., 1993). For the majority of bursts, $\alpha > -2$ and $\beta < -2$, in which case the νF_ν spectrum has a maximum at E_p that represents where the burst emits most of its energy;

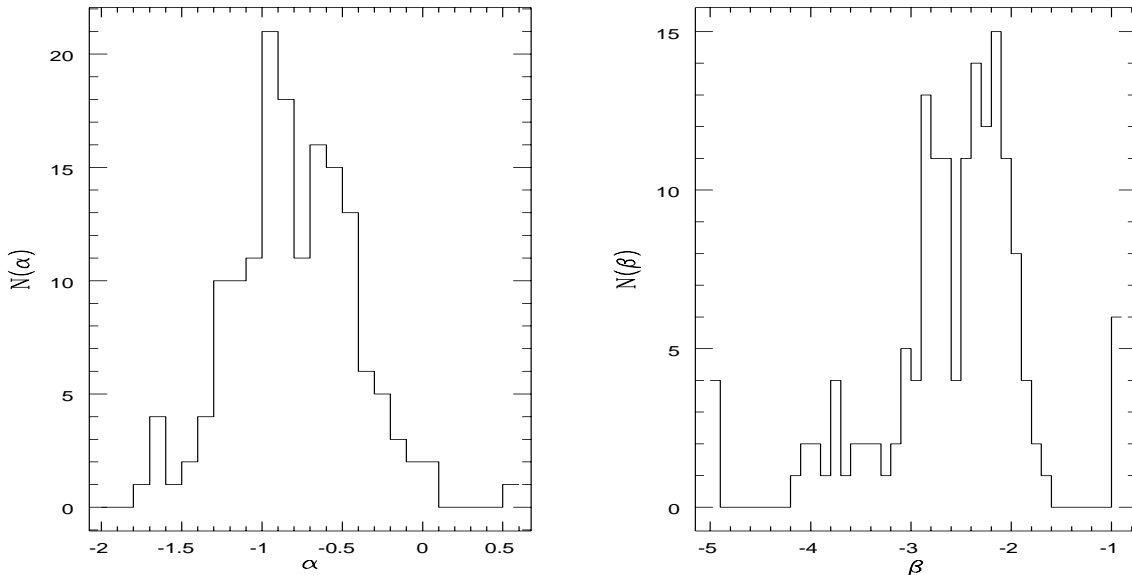


Fig. 1.— Distributions of the low and high energy photon spectral indices α (left panel, $N(\alpha)$) and β (right panel, $N(\beta)$), from Preece et al. (1999).

for a Band spectrum, $E_p = (2 + \alpha)E_b/(\alpha - \beta)$. In most emission models, E_p (or E_b) usually reflects some characteristic *electron* energy. In models of GRB emission with a power law energy spectrum for the radiating particles, it could signify the presence of a cutoff in the underlying particle distribution, or the energy above which all electrons “cool” - rapidly radiating all of their kinetic energy within the source (see Piran, 1999, for a review). The high energy photon index, β , usually reflects the steepness of the particle energy distribution. The value of the low energy photon index, α , on the other hand varies significantly from model to model and can be due to several factors. Therefore, it has greater potential to distinguish between the different scenarios for GRB emission. However, despite years of availability of high quality spectral data from GRBs, the burst emission process remains ambiguous.

It was suggested (e.g. Katz, 1994) that synchrotron emission is a likely source of radiation from GRBs, and later shown (Tavani, 1996) that an *optically thin* synchrotron spectrum from a power law distribution of relativistic electrons with a *sharp minimum energy cutoff* ($N(\gamma) \propto \gamma^{-p}, \gamma > \gamma_m$, where γ is the electron Lorentz factor) and with an *isotropic pitch angle distribution* provides a good fit to some bursts. However, some features seen in the low energy portion of GRB spectra can not be explained by this simple synchrotron model. This model predicts that E_p is related to the minimum value of the electron Lorentz factor, γ_m ($E_p \propto \gamma_m^2 h\nu_B$, where $\nu_B = eB/2\pi m_e c$ is the gyrofrequency in a magnetic field with mean perpendicular component B), so that the asymptotic value of the low energy photon index, α , should be a constant value of $-2/3$ (e.g., Pacholczyk, 1970). Hence, if our spectral fits are determining the asymptote accurately, the α distribution should be a very narrow distribution centered about $-2/3$. Figure 1 shows the time averaged distributions of α and β taken from Preece et al. (1999). The α distribution clearly

appears to disagree with this simple synchrotron model. It has also been claimed (e.g. Crider et al., 1997) that spectral evolution of α (and E_p , for that matter) throughout a burst is inconsistent with the standard synchrotron scenario, at least in the context of a single (external) shock model. Consequentially, other models - usually involving Compton scattering (Brainerd, 1994, Liang & Kargatis, 1996) - are invoked to explain this “anomalous” spectral behavior. Another difficulty with the synchrotron model stems from theoretical considerations. For typical spectral peak energies $E_p \sim \text{few} \times 100 \text{ keV}$, and “typical” values for the electron Lorentz factors $\gamma \sim 100$ and bulk Lorentz factor $\Gamma \sim 100$, magnetic fields can reach values of about $10^7 G$ (such fields are also reached simply assuming equipartition between photon, electron and magnetic field energy density). As a result, the synchrotron lifetime in the observer’s frame ($\tau_s = (\gamma/\dot{\gamma}_s)(1+z)/\Gamma$) $\lesssim 10^{-6} s$, where $\dot{\gamma}_s \propto \gamma^2 B^2$ is the synchrotron energy loss rate, Γ is the bulk Lorentz factor of the medium, and z is the GRB redshift) is much shorter than the physical timescales relevant in the standard fireball model for GRBs (again, see Piran, 1999 for a review), as well as the detector integration time. Thus, one expects these radiative loss effects to be apparent in the GRB spectrum. For example, if the electrons are injected in a source region where those with energies $\gamma > \gamma_c$ lose all their energy to radiation (while those with $\gamma < \gamma_c$ escape the emission region before suffering significant losses of their kinetic energy), then one obtains the so-called *cooling* spectrum which has an additional break at a photon energy $E_c \propto \gamma_c^2 h\nu_B$. Depending on the relative values of γ_m and γ_c , one has a variety of values for the spectral indices. For example, if $\gamma_c > \gamma_{\min}$ (and we have the same power law distribution of electron energy mentioned above) then one has an index $\beta' = -(p+2)/2$ above E_c . In the case when $\gamma_c < \gamma_{\min}$, *all* of the injected electrons lose their energy to radiation and we therefore have an index $\alpha' = -3/2$ between γ_c and γ_{\min} . The peak of the νF_ν spectrum, E_p , could represent either the cooling or the minimum Lorentz factor break, depending on their relative values and their positions in the BATSE spectral window (see, e.g. , Sari, Piran & Narayan 1998). Hence, in a cooling spectrum, we expect either α or β to be about -1.5, which is not borne out by the observations as seen in Figure 1. Ghisellini et al. (1999) use this argument to rule out synchrotron emission in favor of a quasi-thermal inverse Compton model. We agree that the simple cooling spectrum is ruled out by the observations. However, we also believe that this does not rule out synchrotron emission in general, and that all of these above mentioned discrepancies arise from incorrect simplifying assumptions in the models.

Let us first consider the arguments based on the discrepancy with the cooling spectrum. We believe the reason for this discrepancy lies in the artificial separation between particle acceleration and radiation. In this model particles are accelerated in one region, and then either the acceleration processes automatically cease or the particles are injected into another region in which they radiate away all of their energy. We believe that such a model of the particle acceleration and radiation processes is an unrealistic situation. It is likely that both acceleration and cooling or radiation processes take place behind the shock continually throughout the emission episode. The acceleration rate R_{acc} and the synchrotron loss rate $R_{syn} = \gamma/\dot{\gamma}_s$, where $\dot{\gamma}_s$ is defined in the previous paragraph, compete with each other in forming the instantaneous spectrum of the electrons which produces the observed synchrotron spectrum. Since the synchrotron loss increases rapidly with energy, its effect is to inhibit acceleration beyond some maximum value γ_{\max} where the two rates become equal, $R_{acc}(\gamma_{\max}) = R_{syn}(\gamma_{\max})$. Thus, we expect a power law electron

spectrum for $\gamma < \gamma_{\max}$, with a relatively sharp cutoff outside γ_{\max} . In reality, the spectrum of the accelerated electrons could be more complex and may lead to the formation of a plateau just below γ_{\max} or to other features (e.g., see Petrosian & Donaghy, 2000). Considering observations up to the GeV range of some GRBs by the EGRET instrument on CGRO, γ_{\max} must be large enough so that the energy of the corresponding synchrotron photons will far exceed the BATSE range. Thus in this model E_p is related to γ_m , the minimum energy of the accelerated electrons, and not to any cooling break.

We point out that the high energy photon indices for a simple cooling spectrum and the so-called “instantaneous” spectrum (in which cooling effects are negligible) are $-(p+2)/2$ and $-(p+1)/2$, respectively. Observed values of $\beta \sim -2.1$ indicate values of $p \sim 2.2$ for the simple cooling model and 3.2 for the instantaneous spectrum. Recent studies of particle acceleration via the Fermi mechanism in relativistic shocks determine a “universal” index of $p \sim 2.2$ (e.g., Gallant et al., 2000, Guthman et al., 2000), which is more consistent the values expected from the cooling model, and this has been used as an argument against the instantaneous spectrum. However, we note that β is usually not very well constrained by the data and the 1σ errors are frequently of the order $\pm 1/2$, so that observations cannot distinguish between the cooling and instantaneous spectra. Moreover, the cooling spectrum itself is not consistent with the universal index for the significant fraction of bursts with $\beta \lesssim -2.5$. In any case, this universal index is based on a very simplified model; particle acceleration in the context of internal shocks has not been carefully studied, and it is unclear whether the Fermi mechanism will even work at all (see, e.g. Lyutikov & Blackman, 2000 and Kirk et al., 2000, the latter of whom show that including a magnetic field at the acceleration site will steepen this universal index). In most of our analysis below, we will use the instantaneous synchrotron spectrum, and not the simple cooling spectrum; we will show that this instantaneous synchrotron spectrum can indeed explain the behavior seen in the BATSE spectral data.

Another simplification in standard synchrotron models that leads to discrepancies between the theory and the observations is the assumption that the GRB emission region is optically thin. Under certain conditions, the medium may in fact become opaque, e.g. to synchrotron self-absorption (discussed in §2.1). This will produce a steep low energy cutoff in the photon spectrum. This is one possible explanation for those bursts with α values above the so-called “line of death”, $\alpha > -2/3$ (Preece et al., 1998a)

A third unrealistic simplification involves the electron spectrum at low energies. The asymptote of the optically thin photon spectrum $\alpha = -2/3$ is obtained if one assumes that the electron spectrum cuts off sharply below γ_m . It is unlikely that the acceleration process will give rise to such a spectrum, which is subject to plasma instabilities. Particles in front of a relativistic shock - after crossing it - will acquire a Lorentz factor comparable to the bulk Lorentz factor of the shock. Subsequent interaction with the turbulent medium will accelerate them to higher energies (up to γ_{\max} described above), but the same processes will decelerate some to lower energies (see, e.g., Park & Petrosian, 1995, and references cited therein). Plasma instabilities (e.g. the two stream instability) can further smooth this peaked spectrum (and in some cases give rise to a nearly flat spectrum for $\gamma < \gamma_m$). Inclusion of such effects will clearly modify the behavior of the

low energy synchrotron emission.

A fourth assumption in the simple synchrotron model, which may not always be correct, is that the pitch angle distribution of the electrons is isotropic. An isotropic distribution is expected if the acceleration mechanism is more efficient in changing the pitch angle rather than the energy of the particles, which is commonly the case. However, in low density high magnetic field plasmas, the opposite may be true so that a highly anisotropic distribution of pitch angles is expected; as a result, the low energy synchrotron spectrum will differ from the usual simple model. Note that as long as the magnetic field lines have random orientations, the total emission in the rest frame will be isotropic. For details, see Epstein (1973).

In what follows, we will show that incorporating all of these effects can lead to a wide variety of low energy GRB spectral behavior. However, there is another important cause of the discrepancy between the predicted and observed spectral behavior, which arises as a result of the finite bandwidth of the instrument and the spectral fitting procedure. One cannot assume that the spectral fits to phenomenological models are able to accurately determine the asymptotic values of the spectral indices. This is because the actual spectra do not show sharp breaks at E_p (or E_b) from the high energy spectral index to the low energy spectral index - rather, there is a smooth transition between the two indices. The fitted values of the low energy (and high energy, for that matter) spectral index depends on how far the spectral window extends below (or above) E_p . We must take these effects into consideration when testing any model.

In this paper we show that when these procedural effects as well as more realistic synchrotron models are incorporated, synchrotron radiation can accommodate both the shape of the distributions and temporal evolution of GRB spectral parameters, and the discrepancies discussed above are resolved. Of course this does not *prove* the synchrotron model is the unique emission mechanism for GRBs, but merely shows that it is consistent with the existing data. In §2, we discuss the various spectral shapes obtained from a general form for synchrotron emission, allowing for the possibility for self-absorption, a smooth (instead of sharp) cutoff to the electron energy distribution, and a small pitch angle distribution. In §3, we consider the instrumental and fitting effects and point out a correlation that exists between α and E_p as determined by the Band spectrum (Band, 1993). In §4, we use this relationship and knowledge of the E_p distribution to determine the expected α distribution, and compare this with the observed distribution. We also discuss the presence of an absorption cutoff and evidence of small pitch angle scattering observable by BATSE in some GRBs to explain particularly those bursts with $\alpha > -2/3$. These results also predict a certain relationship between α and E_p during the temporal evolution of a GRB. In §5, we give examples of spectral evolution in GRBs and discuss whether these are consistent with synchrotron emission models. A summary of our conclusions are given in §6.

2. Synchrotron Spectra

Synchrotron radiation will occur when relativistically charged particles have a component of their velocity perpendicular to a local magnetic field (i.e. a non-zero pitch angle). The importance

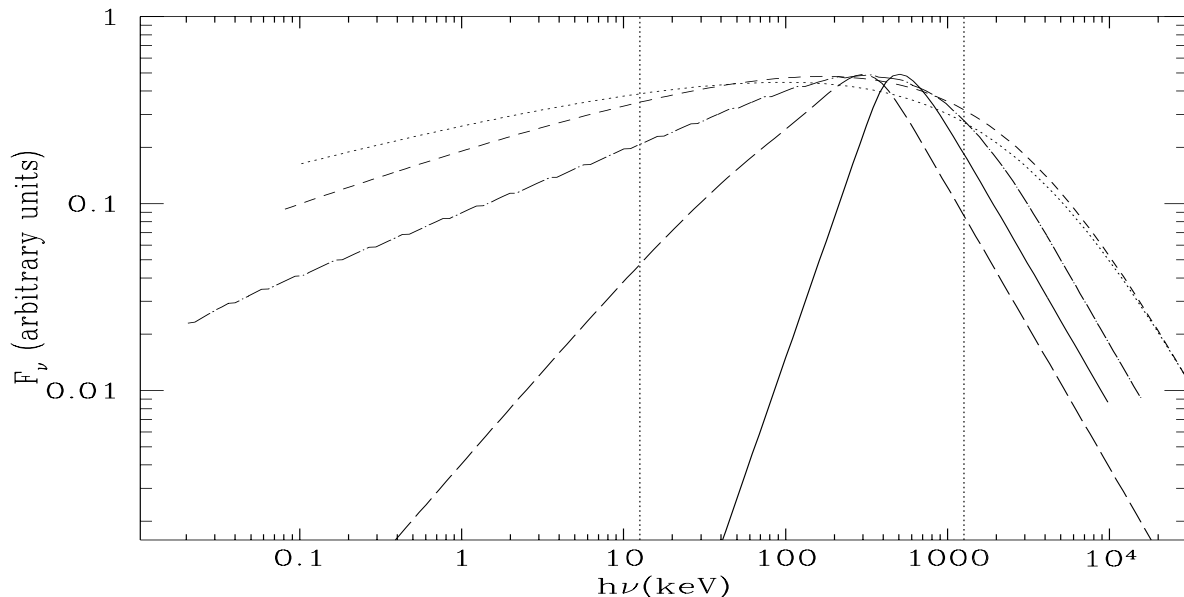


Fig. 2.— Various synchrotron energy spectra, F_ν (in arbitrary units), as a function of energy $h\nu$ in keV. The dot-dashed line is the usual simple optically thin spectrum (with a sharp cutoff to the electron distribution, $q \rightarrow \infty$), while the dotted and short-dashed lines show optically thin spectra for $q = 0$ and $q = 2$ cutoffs respectively; all of these are for an isotropic electron pitch angle distribution. The solid line and long dashed lines show a self-absorbed spectrum for $\nu_a > \nu_m$ and the small pitch angle distribution case, respectively. The vertical lines mark the approximate width of the BATSE spectral window. The spectra are normalized at their peaks to some representative value and all have the same value of the high energy spectral index, $p = 4$.

of synchrotron emission (compared to, say, inverse Compton or brehmstrahlung radiation) depends - among other things - on the strength of the magnetic field. Given the relativistic nature of GRBs and probable physical conditions (e.g. significant magnetic fields), it is likely that synchrotron radiation plays a role in the emission from GRBs. The general form for an instantaneous synchrotron *energy* spectrum from electrons with a (homogeneous) power law distribution of Lorentz factors with a sharp cutoff, $N(\gamma) = N_0 \gamma^{-p} \Theta(\gamma - \gamma_m)$ (where Θ is the Heaviside step function), and with an isotropic pitch angle distribution, is given by (e.g. Pacholczyk, 1970)

$$F_\nu = \mathcal{A} \nu^{5/2} \left[\frac{I_1}{I_2} \right] \times [1.0 - \exp[-Q \nu^{-(p+4)/2} I_2]] \quad (1)$$

$$I_1 = \int_0^{\nu/\nu_m} dx x^{(p-1)/2} \int_x^\infty K_{5/3}(z) dz \quad (2)$$

$$I_2 = \int_0^{\nu/\nu_m} dx x^{p/2} \int_x^\infty K_{5/3}(z) dz, \quad (3)$$

Here, we have assumed that the electrons are extremely relativistic, $\gamma_m \gg 1$, and that the magnetic field at the source is randomly oriented, or that the emission is isotropic. The coefficient \mathcal{A} is the normalization and contains factors of the magnetic field, B , bulk Lorentz factor, Γ , and

electron number, N_o . The integrand $K_{5/3}(z)$ is a modified Bessel function of order $5/3$. The parameter $\nu_m = ((3/2)\Gamma\gamma_m^2\nu_B)$, and Q is proportional to the optical depth (to self-absorption) of the medium; for $\nu \gg \nu_m$, the photon spectrum is self-absorbed at $\nu < \nu_a \propto Q^{2/(p+4)}$. The high energy optically thin asymptotic behavior is the usual $F_\nu \propto \nu^{-(p-1)/2}$. The low energy asymptotic forms of the function depend on the relative values of ν_m and ν_a : $F_\nu \propto \nu^{5/2}$ for $\nu_m < \nu \ll \nu_a$, but is much flatter - $F_\nu \propto \nu^{1/3}$ - for $\nu_a < \nu < \nu_m$. For very low frequencies, $\nu \ll \min[\nu_a, \nu_m]$, $F_\nu \propto \nu^2$. We point out that the *photon* spectral index α is $d\log(F_\nu)/d\log(\nu) - 1$. Figure 2 shows the many different types of low energy behavior one can obtain from synchrotron emission. The dot-dashed line is the usual simple optically thin spectrum, and the solid line shows a self-absorbed spectrum for $\nu_a > \nu_m$. The dotted and short dashed lines show optically thin spectra for a gradual (rather than sharp) cutoff to the electron distribution, discussed in §2.2. The long dashed line shows a spectrum in the case of small pitch angle scattering, discussed in §2.3. Since we are focusing on the low energy spectral index α , we have kept β constant and normalized the spectra at their peaks to a representative value within the BATSE window approximated by the vertical dotted lines.

2.1. Synchrotron Self Absorption

Most treatment of synchrotron radiation from GRBs has been in the optically thin case (see, however, Papathanassiou, 1998). This is because synchrotron self-absorption requires “extreme” physical conditions in a GRB - particularly, high magnetic fields and a high column density of electrons. For example, for $\nu_a < \nu_m$, the optical depth to synchrotron self absorption is $\tau \sim (l/10^{13} \text{ cm})(n/10^8 \text{ cm}^{-3})(B/10^8 \text{ G})^{2/3}(\gamma_m/50)^{-8/3}(\Gamma/10^3)^3(\nu_{obs}/10^{19} \text{ Hz})^{-5/3}$, where l and n are the path length and particle density in the co-moving frame, ν_{obs} is the absorption frequency in the observer’s frame (note that this frequency falls within BATSE’s spectral window), and we have assumed an electron energy distribution index $p = 2$. For a more detailed discussion of absorption frequencies in various regimes, see Granot et al., 2000. An example of a self-absorbed spectrum is given by the solid line in Figure 2. As evident from the above expression, optical depths of order unity can be achieved within the BATSE spectral range with somewhat extreme values of the physical parameters, most notably the value of the magnetic field. However, such high values of the magnetic field can be reached simply through equipartition in internal shocks (see, e.g., Piran, 1999). In general, we understand far too little about the generation of magnetic fields and the hydrodynamical conditions relevant for GRBs to rule out these extreme physical parameters. We also point out that the required values of n , l , and γ_m lead to a Compton Y parameter of order unity or greater, thereby reducing the efficiency of synchrotron radiation in the observed range (Kumar, 1999, Piran, 1999). In this paper, we do not focus on how the conditions required for observable synchrotron self-absorption are achieved, but rather investigate the consequences if they indeed are reached. In any case, as shown in Figure 1 above and as we will see below, a self-absorbed spectrum may be applicable to only a small fraction of the GRB population.

To test how well the optically thin and thick synchrotron spectra fit the data, we fit 11 bursts with 256 channel energy resolution to the synchrotron spectral form in equation (1). In six cases,

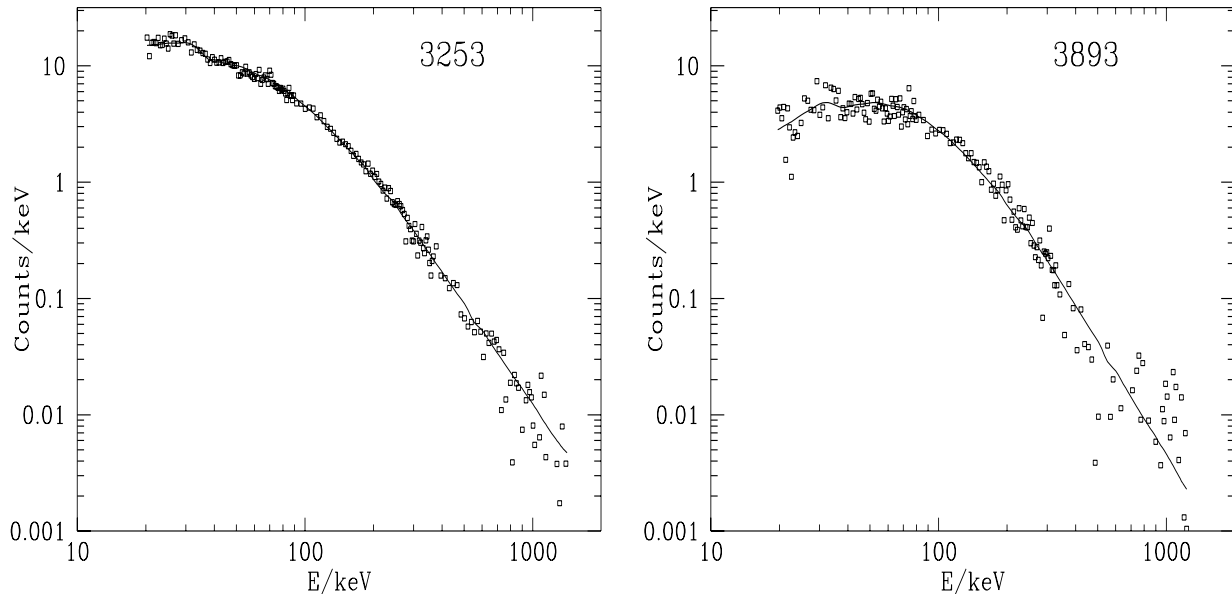


Fig. 3.— Synchrotron fits to photon spectra of BATSE GRBs with trigger numbers 3253 (left panel) and 3893 (right panel). We display the count spectrum, which is the photon spectrum, convolved with the detector response matrix. An optically thin spectrum with $h\nu_m = 44$ keV gives the best fit to 3253, while an optically thick (to synchrotron self-absorption) spectrum with $h\nu_m = 52$ keV and $h\nu_a \approx 40$ keV best fits 3893.

the *optically thin* spectrum fit the bursts well. But for five bursts, which have a low energy photon index $\alpha > -2/3$ (as determined by fitting a Band spectrum, Preece et al., 1999), the optically thin spectrum does not provide a good fit. For these bursts, we find that when including a parameter characterizing the optical depth (Q in equation 1), *the fits are improved significantly over those to the optically thin spectra*. Crider & Liang, 1999, also show self-absorption is consistent with GRB 970111, another burst with a hard low energy spectral index ($\alpha > -2/3$). It should be noted, however, that in all of these bursts, $\nu_m > \nu_a$, and ν_a was close to the edge of the BATSE window (in fact, the presence of only a few bursts with $\alpha = 1$ or $3/2$ (see Figure 1) indicates that in general $h\nu_a \lesssim 50$ keV). We discuss the implications this has on the observed α distribution below. Figures 3a and 3b show the spectral fits for 2 GRBs in our sample (burst triggers 3893 and 3253). An optically thin spectrum is the best fit to 3253, while a self-absorbed spectrum is required for 3893 - the rollover at low energies expected from synchrotron self-absorption is evident, and clearly cannot be accommodated by an optically thin spectrum. [Note that these are *counts* spectra and not photon spectra, so the bumps in the data and the model are a result of the convolution of the impinging photon spectrum and the model convolved with the detector response matrix.]

2.2. The Electron Energy Spectrum

In most models of synchrotron emission, the electron distribution is modeled by a power law with spectral index p (as done above). Since the high energy index $\beta = -(p + 1)/2$ (or $-(p+2)/2$ for a simple cooling model), and the majority of bursts have $\beta > -1.5$ (see Figure 1), this means that the index $p > 2$. As a result, a cutoff to the power law distribution at some minimum energy γ_m must be imposed to prevent divergence of the accelerated electron energy distribution at low energies. However, as discussed in the introduction, such a sharp cutoff is not a realistic - even stable - scenario. Instead, one expects to produce a gradual cutoff to the electron distribution (perhaps due to such effects as the two stream instability). In general, particle acceleration in relativistic shocks is not well understood, and could produce a range of low energy power law tails (among more complicated behavior) to the electron distribution, or even a nearly flat low energy electron spectrum. In order to account for this range of possible low energy behavior, we characterize the electron distribution by the following equation:

$$N(\gamma) = N_o \frac{(\gamma/\gamma_m)^q}{1 + (\gamma/\gamma_m)^{p+q}} \quad (4)$$

where, now, γ_m is some critical energy below which the electron distribution changes from p to q . For $\gamma \gg \gamma_m$, $N(\gamma) \propto \gamma^{-p}$, while for $\gamma \ll \gamma_m$, $N(\gamma) \propto \gamma^q$. Hence, q characterizes the “smoothness” of the cutoff (note for $q \rightarrow \infty$, γ_m becomes a sharp cutoff to the distribution as defined in the previous section).

For this new electron distribution, an optically thin synchrotron spectrum for an isotropic pitch angle distribution takes the form:

$$F_\nu = \mathcal{C}(\nu/\nu_m)^{(q+1)/2} \int_0^\infty dx \frac{x^{-(q+1)/2}}{1 + ((\nu/\nu_m)^{(q+p)/2} x^{-(p+q)/2})} \int_x^\infty K_{5/3}(z) dz \quad (5)$$

where, again, $\nu_m = (3/2)\Gamma\gamma_m^2\nu_B$, and \mathcal{C} is the normalization. Note that for $q < -1/3$, the asymptotic photon index $\alpha = \frac{q+1}{2} - 1 < -2/3$, but for $q > -1/3$, this index $\alpha = -2/3$. This simply means that for $q < -1/3$, the superposition of the photon spectra from individual electrons below γ_m becomes powerful enough to change the low energy behavior. That is, there is a “competition” between $\nu^{1/3}$ (the low energy photon spectrum for an individual electron) and $\nu^{(q+1)/2}$ (the superposed low energy behavior of the electron distribution below γ_m) - when $(q + 1)/2 < 1/3$, the low energy behavior below ν_m is different than the usual $\nu^{1/3}$. Nonetheless, even for $q > -1/3$, the “smoothness” of the cutoff can change the spectrum of the emitted photons significantly, primarily making the transition from the high energy index β to the low energy asymptotic value of $\alpha = -2/3$ more gradual. Examples of spectra with $q \neq \infty$ are shown in Figure 2 by the dotted ($q = 0$) and short dashed lines ($q = 2$). We point out that as the cutoff of the electron distribution is made smoother (q smaller), the peak of the spectrum shifts to lower energies, while the asymptotic value of the spectral index is approached at a slower rate. Figure 4 shows both of these effects. The solid line shows the peak of the F_ν spectrum, denoted as $h\nu_{max}$, as a function of q ; the dotted line shows the ratio of $h\nu_{max}$ to $h\nu_{asympt}$, where $h\nu_{asympt}$ is defined as the energy in which the optically thin spectral index is within 5% of its low energy asymptotic value of $1/3$.

2.3. Small Pitch Angle Emission

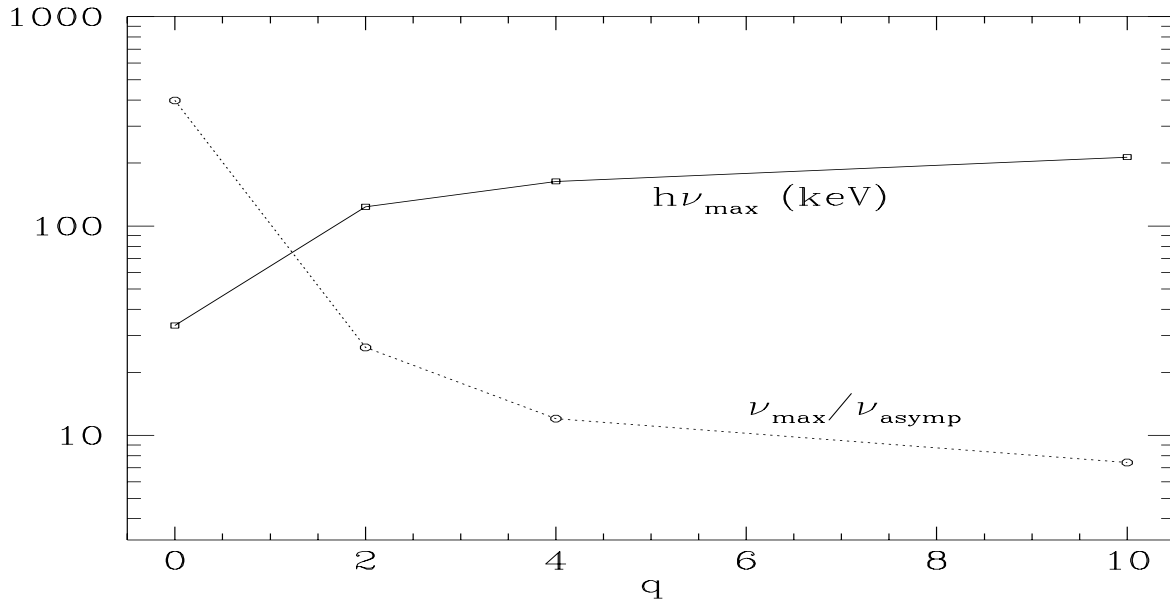


Fig. 4.— The peak of the F_ν spectrum, $h\nu_{\max}$, as a function of q (solid line), and the ratio of $h\nu_{\max}$ to $h\nu_{\text{asymp}}$ (dotted line) where $h\nu_{\text{asymp}}$ is defined as the energy in which the optically thin spectral index is within 5% of its low energy asymptotic value of $1/3$. Note that the dependence on q for the latter curve is quite strong for $q \lesssim 3$, the smoothest cutoffs.

The usual analysis of synchrotron radiation assumes electrons are distributed isotropically in a either a uniform or randomly oriented magnetic field geometry (Pacholczyk, 1970). However, this is a simplifying assumption and sometimes one expects a non-isotropic pitch angle distribution, usually beamed along the field lines. If the beaming is strong so that most electrons have pitch angles $\theta < 1/\gamma$ (the Lorentz factor of the electron), the shape of the synchrotron spectrum changes significantly (see Epstein, 1973, and Epstein & Petrosian, 1973). An efficient method of producing isotropic pitch angle distributions at relativistic energies is by plasma turbulence, which can scatter and change the energy of the electrons. For high density, low magnetic field plasmas the Alfvén phase velocity is less than the speed of light and therefore the speed of the particles (relativistic in our case). In this case, the pitch angle diffusion rate of the electrons interacting with plasma turbulence is much larger than the acceleration rate; consequently, the accelerated electrons will have an isotropic pitch angle distribution. However, for the low density, high magnetic field condition expected for the sources of GRBs the opposite is true. In this case the fluctuation in the electric field of the waves exceeds the fluctuation of the magnetic field so that the above situation is reversed (see e.g. Dung & Petrosian, 1994 or Pryadko & Petrosian 1997). Then the pitch angle distribution of the accelerated electrons could become highly anisotropic as required in the small pitch angle model. One consequence of a small pitch angle distribution is that the resulting spectrum at low frequencies is approximately: $F_\nu \propto \nu$, for $\nu < \nu_s$, where ν_s characterizes the where small pitch angle scattering is important. Above this frequency, F_ν follows the usual synchrotron spectrum (again, we have assumed that $\theta\gamma \ll 1$, where θ is the electron pitch angle. This leads to a single particle emissivity that goes as ν up to $2\gamma\nu_B$, and sharply cuts

off after that; see Epstein, 1973, §II). An example of a synchrotron spectrum with a small pitch angle distribution in this regime is shown by the long dashed line in Figure 2. Note that this is an optically thin spectrum with $\alpha = 0$; this is above the so-called “line of death” $\alpha = -2/3$. It should be noted that a very similar low energy spectrum is obtained when an *isotropic* distribution of electrons is embedded in a region with a very tangled magnetic field. If there exist magnetic field fluctuations with a correlation length that is less than the Larmor radius of the electrons, then there will be transverse deflections of the electrons with angles less than the relativistic beaming angle. Emission due to these fluctuations is very similar to the small pitch angle case and therefore also produces a spectrum $F_\nu \propto \nu$ at low energies (Medvedev, 2000). Note that the latter scenario imposes restrictions on the structure of the magnetic field, while the former (small pitch angle) model constrains the acceleration mechanism.

3. The Low Energy Asymptotic Behavior

We have shown so far that synchrotron emission can result in low energy spectral index values of $\alpha = d\log(F_\nu)/d\log(\nu) - 1 = -2/3, 0, , 1.5$ (and possibly -1.5 if “cooling” effects are important). The observed distribution shown in Figure 1, on the other hand, shows a broad and continuous distribution of α with about 96% of bursts in the range $-1.5 < \alpha < 0$. We propose that this dispersion is caused by the finite bandwidth of the BATSE instruments and arises from the fitting of a phenomenological model to the data. The theoretical values stated above represent the asymptotic logarithmic slopes far from the break or peak photon energy. How well a fitting algorithm can determine these asymptotic values depends on whether the asymptotic value of the spectrum is reached within the detector window. This depends both on how “quickly” the spectrum reaches its asymptote and the value of E_p relative to the lower end of the detector window. In other words, we need to understand how well spectral fits can determine the low energy asymptote for the different cases presented above. For example, as E_p moves to lower and lower energies, we get less and less of the low energy portion of the spectrum; in this case, our spectral fits probably will not be able to determine the asymptotic index and will measure a smaller (softer) value of α . Preece et al. (1998a) pointed out this effect and attempt to minimize it by defining an effective low energy index, α_{eff} , which is the slope of the spectrum at 25keV (the edge of the BATSE window). However, a correlation between α_{eff} and E_p will still exist if the asymptotic value is not reached by 25keV. This difficulty becomes more severe the smoother the cutoff to the electron distribution, because the spectrum takes longer to reach its asymptotic index.

To determine the extent of these effects, we simulated data from optically thin synchrotron models with different values of the parameters ν_m and q (which determine the values of E_p and α in a Band spectral fit). We have included spectra both for an isotropic pitch angle distribution and for a distribution of electrons having small pitch angles only. Note that since we take an optically thin spectra with $q \geq 0$, all of the spectra have a low energy asymptote of $-2/3$ (isotropic pitch angle distribution) or 0 (small pitch angle distribution). We normalize the spectra so that

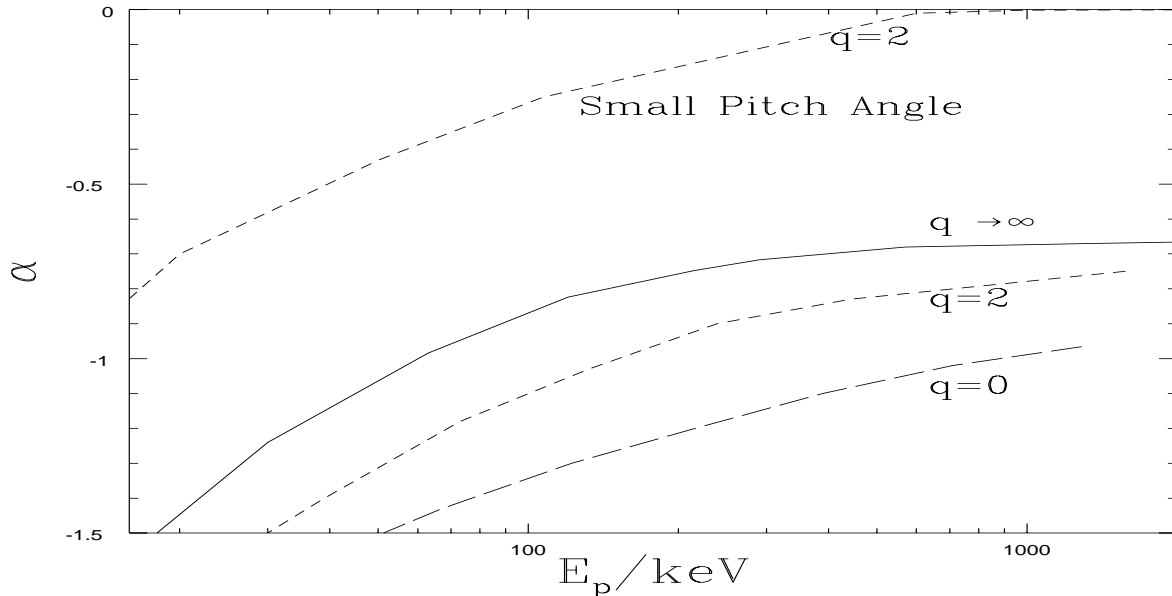


Fig. 5.— The low energy photon index α vs. E_p , the peak of νF_ν , for optically thin spectra with different values of q for an isotropic pitch angle distribution (lower three curves), and a small pitch angle distribution (upper curve). The values of q (smoothness of electron spectrum cutoff) are labeled. Note that the smoother the cutoff the electron energy distribution (lower q) the longer it takes the spectrum to reach the optically thin asymptote within the BATSE window.

the peak photon flux in the range 50 – 300 keV is 10ph/cm²/s (e.g. a fairly bright GRB). Our data points are then drawn from a Poisson distribution with a mean at the value given by the synchrotron photon spectrum at a particular frequency; that is, the data points are drawn from a Poisson distribution with a mean $N_{\nu,i} = (F_\nu/h\nu)_i$, where i indexes the data point. We then fit a Band spectrum to this data using a conservative estimate that BATSE is sensitive to all photons above 10 keV. Figure 5 shows the value of α as a function of E_p , for different degrees of the smoothness of the electron energy distribution cutoff in the isotropic pitch angle case (three lower curves), and for an intermediate cutoff in the small pitch angle distribution case (upper curve). Not surprisingly, there is a strong correlation between the value of E_p and the value of the index, α . To make sure this isn't purely an artifact of the Band function, we also tried a broken power law fit ($A(E) \propto E^\alpha$, $E < E_{break}$, $A(E) \propto E^\beta$, $E > E_{break}$, where A is in photons/cm²/s/keV) to our simulated data and found a very similar relationship (although the power law does not give as good of fits as the Band spectrum, so the relationship was noisier). Because GRBs have a relatively broad distribution of E_p , the above correlation between α and E_p will lead to a dispersion in the distribution of α ; to determine the extent of this effect, we need the distribution of E_p 's. In our analysis, we use the distribution observed by BATSE, plotted in Figure 6 (solid line). Note that there has been some controversy over the dispersion in this distribution and we have shown (Lloyd & Petrosian, 1999) that indeed this distribution suffers from selection effects in the BATSE spectral window that tend narrow the it. These effects are evident in Figure 6, which also plots E_p distributions observed by SMM (sensitive to higher energies than BATSE;

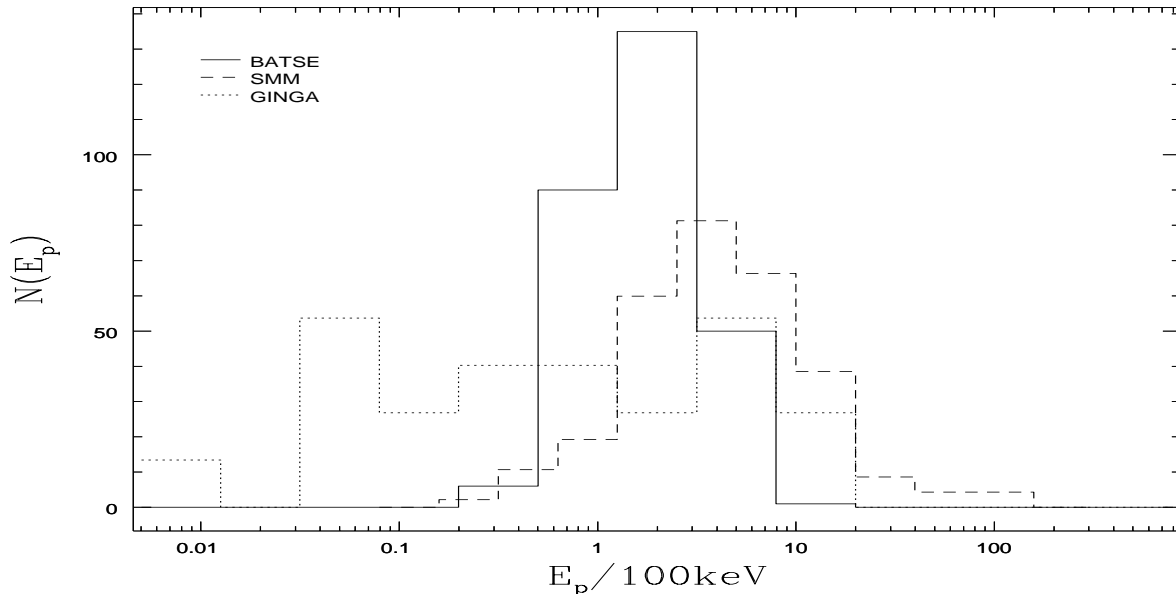


Fig. 6.— The superposed BATSE, SMM, and GINGA E_p distributions, $N(E_p)$.

Harris & Share, 1998) and GINGA (sensitive to lower energies than BATSE; Strohmeyer et al., 1998). The former extends the BATSE E_p distribution on the upper end, while the latter extends it on the lower end. However, we are interested in the BATSE *observed* α distribution through its relationship with the BATSE *observed* E_p distribution. Hence, the intrinsic E_p distribution (with selection effects accounted for) - although relevant for understanding other physical aspects of the radiation processes - is not relevant for our discussion of the observed α distribution.

4. The Observed α Distribution

From the observed distribution of E_p (Figure 6, solid histogram), we can determine how the correlation between E_p and α introduced by the fitting procedure (Figure 5) “smears” the distribution of α away from the expected narrow distribution around the physical asymptotes of $-2/3$, 0 , etc.. We represent the correlation between α and E_p by an approximate simple analytical function; $\log(E_p) = h(\alpha)$, where the function $h(\alpha)$ depends on the specifics of the synchrotron model (see Figure 5). We then approximate the E_p distribution, $f(\log(E_p))$ by a Gaussian in $\log(E_p)$, with a mean and dispersion equal to those of the observed distribution. The distribution of α is then obtained from the relation

$$g(\alpha) = f(\log(E_p)) \frac{dh(\alpha)}{d\alpha}. \quad (6)$$

Figure 7 shows the resultant α distributions in the case of an isotropic pitch angle distribution for a sharp ($q = \infty$, right solid curve), intermediate ($q = 2$, middle short-dashed curve), and flat

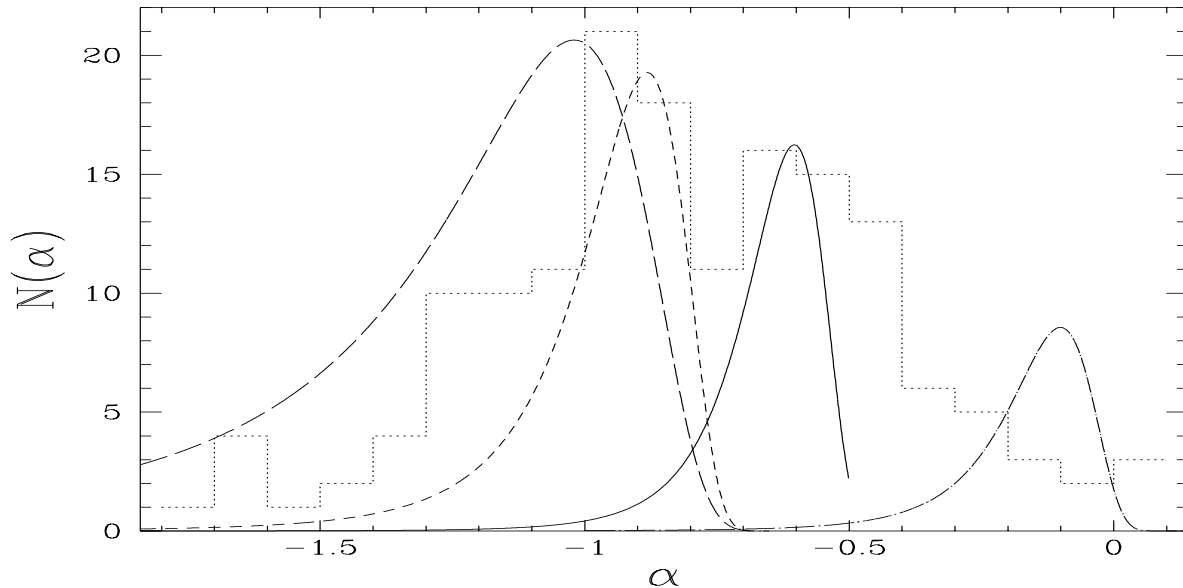


Fig. 7.— The predicted α distributions, $N(\alpha)$, given the the relationships between α and E_p shown in Figure 5. The three left curves are for an isotropic pitch angle distribution for a $q \rightarrow \infty$ (right solid curve), $q = 2$ (middle short-dashed curve), and $q = 0$ (left long-dashed curve) cutoff to the electron distribution, while the rightmost curve is the small pitch angle distribution case for an intermediate cutoff (dot-dashed curve). The dotted histogram is the observed distribution taken from Preece et al. (1999) also shown in Figure 1. The simulated curves have been separately normalized to the height of this observed distribution.

($q = 0$, left long-dashed curve) cutoff to the electron energy spectrum, as well as the small pitch angle distribution case for an intermediate cutoff (right dot-dashed line). The dotted histogram is the observed α distribution shown in Figure 1. The simulated curves have been arbitrarily normalized to the height of the observed distribution at their central values of α . We note the following:

1) It appears that almost the entire range of the observed distribution can be covered by these optically thin synchrotron models. In particular, given a distribution in q , an instantaneous optically thin spectrum in the large pitch angle scattering regime can easily accomodate bursts below the “line of death” with $\alpha \lesssim -2/3$, where most of the bursts are located.

2) The second conclusion is that the electron energy distribution below the turnover energy γ_m must be falling off, or must be (at most) flat ($q \geq 0$). Otherwise, the optically thin model would predict too many bursts with α less than about -1.5 .

3) We have shown than an optically thin spectrum from a small pitch angle distribution and a smooth cutoff to the electron energy distribution can explain all bursts with $-2/3 \lesssim \alpha \lesssim 0$.

4) However, this is not necessarily the only explanation. Bursts with $\alpha > -2/3$ all the way up to $3/2$ can also be due to absorption effects. As shown in §2, for some bursts synchrotron

self-absorption is necessary to provide a good spectral fit to the data. However, we usually do not see the values $\alpha = 3/2$ ($\nu_m < \nu \ll \nu_a$) or $\alpha = 1.0$ ($\nu \ll \min[\nu_m, \nu_a]$) expected from self-absorption (there are, however, some bursts with such sharp breaks; see Preece et al., 1999). If self-absorption is important, $h\nu_a$ must be near the lower edge of the BATSE spectral window. In this case, we just begin to see the absorption cutoff and the steep asymptotic low energy slopes are not yet reached. Indeed, this is the case for the fits mentioned in §2.

5) The analysis above becomes more complicated when there are two or more spectral breaks in the detector bandpass (there is some evidence for two breaks in GRB spectra; see Strohmeyer et al., 1998). In this case, a fit to a phenomenological model with a single break will lead to averaging of the slopes above and below the break it did not fit. For example, if ν_m and ν_a are both present in the spectral window with $\nu_m > \nu_a$ and the fit places $E_p \propto \nu_m$, then the Band function will not accomodate the additional absorption break. As a result, the low energy index ends up being a weighted average of the optically thin ($-2/3$) and optically thick (1) indices. If the fit places $E_p \propto \nu_a$, then the high energy index β will be an average of $-2/3$ and $-(p+1)/2$. This of course applies to any other two (or more) characteristic frequencies as well.

6) It should also be noted that we have included only a small amount of noise (from counting statistics) in our simulations - adding more noise will contribute to the spread in the simulated α distributions and strenghten our arguments.

7) Finally, we note that other effects such as inhomogeneities in the electron distribution (Granot et al., 2000) an other radiative transport effects (Grusinov & Meszaros, 2000, Dermer & Boettcher, 2000) can also produce spectra both below and above the values of $\alpha = -2/3$.

5. Spectral Evolution

Not only do emission models have to accomodate the shape of the observed distributions, but also the temporal behavior of the spectral parameters. The behavior of the spectral characteristics with time throughout a GRB can give us information about the environment of the local emission region and conceivably constrain the emission mechanism. If the above interpretation of the α distribution is correct, then we expect considerable correlation between the variation of the observed values of α and E_p throughout a burst. Many studies have looked at time evolution of spectral parameters (e.g. Norris et al., 1986, Ford et al., 1995, Crider et al., 1997, Preece et al., 1998(b)). Ford et al. analyze the evolution of E_p for 37 bright, long duration GRBs observed by BATSE. This study presents evidence of a general envelope of “hard-to-soft” evolution of E_p throughout the duration of the burst. The behavior is explained in the context of an external shock model in which there is a gradual decline of average energy as more particles encounter the shock; the emission mechanism is unspecified. Crider et al. investigate the behavior of the low energy spectral index α for a sample of 30 BATSE GRBs. They find that 18 of these bursts show hard-to-soft evolution, while 12 exhibit so-called “tracking” behavior - when the evolution of α correlates with the burst time profile. All of these bursts also show a strong correlation between α

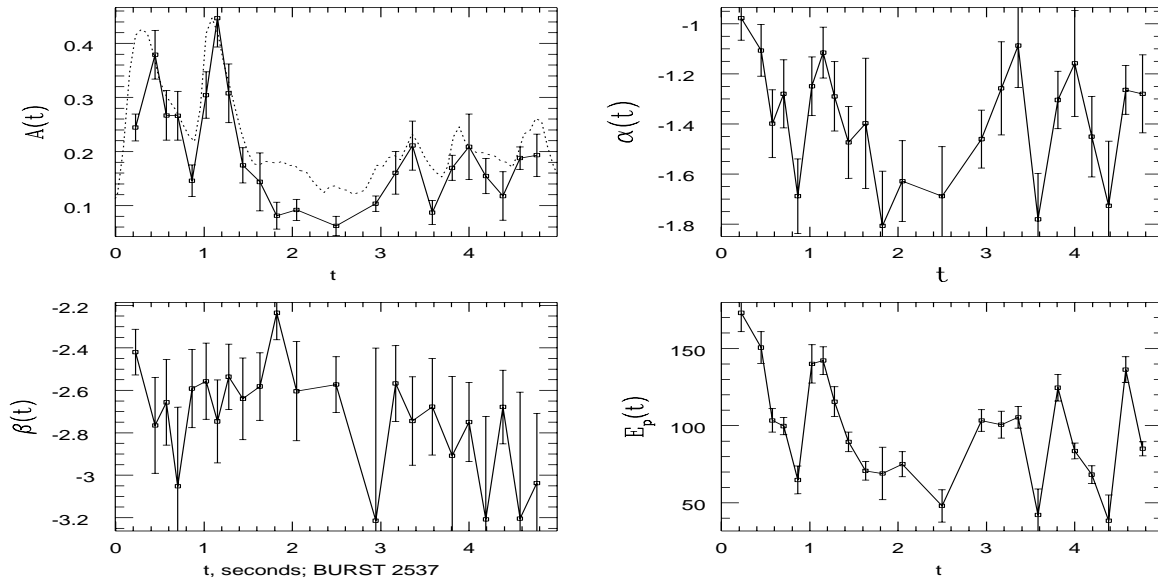


Fig. 8.— Temporal evolution of the four parameters characterizing a Band spectral fit - the low energy photon index α (top right corner), the normalization A in units of photons/cm²/s/keV (top left corner), the high energy photon index β (bottom left corner), the peak energy E_p (bottom right corner) for burst 2537. The time profile of the GRB with with 64ms time resolution (and arbitrary normalization) is the dotted line superimposed on the normalization curve.

and the peak energy, E_p , as a function of time. The authors attribute the hard to soft behavior is to Thomson thinning of a Comptonizing plasma. The “tracking” behavior is not explained.

Recently, Preece et al. (1999) published a catalog of spectral data with high time resolution fitting. We present the time evolution of three of these bursts (Figures 8, 9, and 10), plotting all of the variables that parameterize the (Band) spectral fits. Starting in the upper left hand corner and going clockwise we plot the evolution of the normalization $A(t)$ (in units of photons/cm²/s/keV), α , E_p , and the high energy photon index β . [We point out that the time resolution of the spectral fitting is sometimes coarser than the real time variation of the burst (at least on the shortest detector timescale (64ms)). This will lead to some averaging effects which may weaken the correlation we expect. We have included the higher resolution time profiles (in arbitrary units) superposed on the plot of the normalization $A(t)$, as a reference.] Given the expected correlation between α and E_p from instrumental and fitting procedural effects discussed in the previous section, we expect evolution of α to some extent mimic the evolution of E_p in time.

Indeed this is what we see in Figure 8 - the parameter α “tracks” E_p (and both of these track the flux, A). Note the values of E_p and α are consistent with the case of a flat ($q = 0$) cutoff to the electron distribution, but there may be indication of variation of q as well.

However, it is not always this simple. In an internal shock scenario, we can regard each pulse in the time profile as a separate emission episode; in this case, the internal parameters

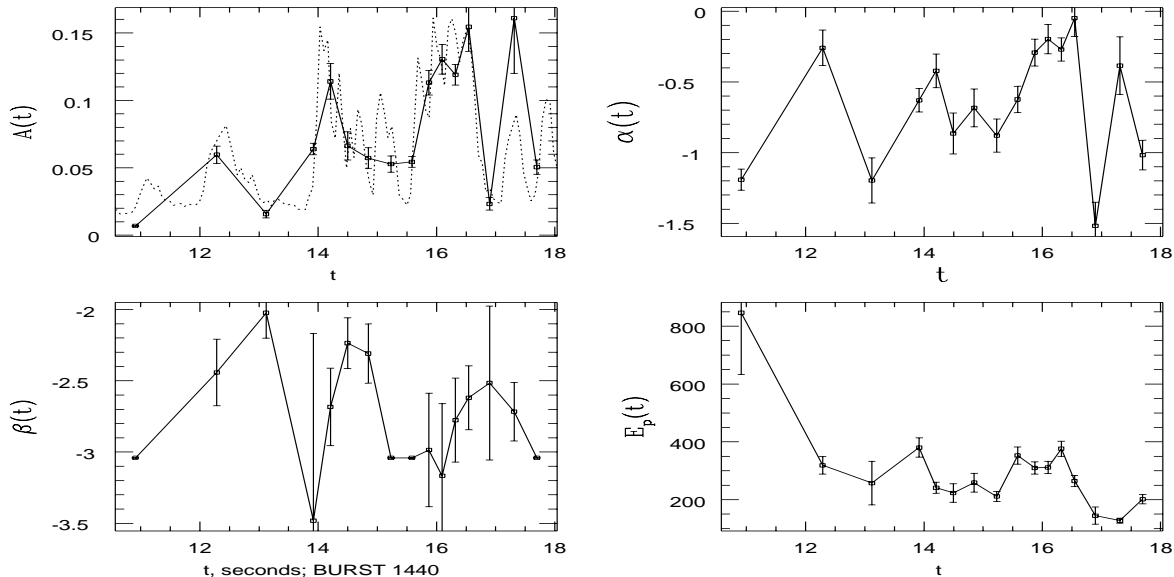


Fig. 9.— Same as Figure 8, but for BATSE trigger number 1440.

can vary depending on the physical conditions at each shock. In particular, a change in q can create a change in α from pulse to pulse, independent of E_p (although we might expect some anti-correlation with E_p in this case - high q gives a high α , but decreases E_p if all other parameters are the same). Figure 9 shows such behavior. The parameter α tracks the flux; E_p varies on the same timescale as the flux, but these variations are superimposed in an envelope of hard-to-soft evolution. This can be explained by a sharpening of the cutoff of the electron distribution from peak to peak. That is, in the first peak, we have fairly high E_p values (~ 500 keV) and moderately low (~ -1) values of α . This is what we expect for a $q \sim 0$ or 1 cutoff. In the second peak, E_p is about 300 keV, but the α value is around -0.6 - this is what we'd expect for a sharper cutoff ($q \gtrsim 5$).

In addition, we may see evidence of evolution of the opacity or pitch angle distribution from pulse to pulse. For example, in Figure 10, the parameter α appears to evolve from hard (above the “line of death”) to soft, while E_p appears to track the normalization. In the early phase, $\alpha > -2/3$ and E_p is moderate (~ 300 keV). At later times, E_p is at fairly high values ($\gtrsim 500$ keV), while α is fluctuating around the expected asymptote for optically thin emission, $\alpha = -2/3$ (this is what we expect from the correlation discussed in this paper - when E_p is high enough, the asymptote of the spectrum is reached inside the BATSE window). The overall behavior can be attributed either to a transition from a small pitch angle to isotropic regime, or to a transition from an optically thick (to synchrotron self-absorption) to optically thin regime. Note that we have not accounted for any biases determination of the high energy photon index β might cause. This ultimately can affect the value of α or E_p . For most cases, β remains fairly constant, with only minor fluctuations.

Our purpose here is not to present a rigorous temporal analysis of the spectral parameters,

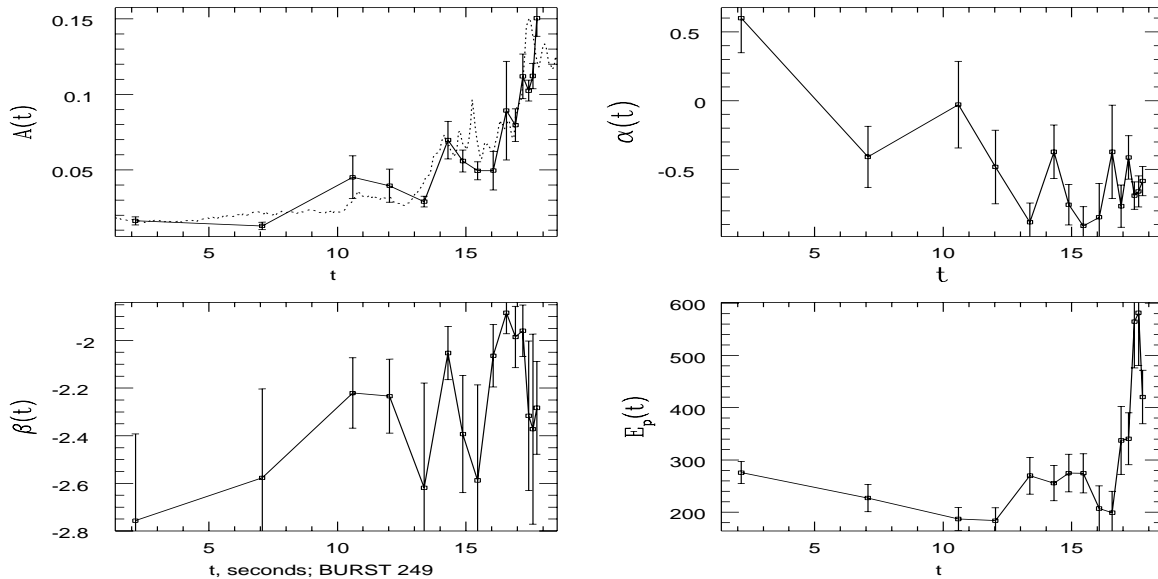


Fig. 10.— Same as Figure 8, but for BATSE trigger number 1440.

but to show the diversity of spectral evolution from burst to burst, and to discuss both the procedural (i.e. spectral fitting) and physical reasons that produce this behavior. The variety of observed spectral evolution and its meaning in terms of synchrotron emission from internal shocks will be discussed in much more detail in an upcoming publication.

6. Summary and Conclusions

Although synchrotron radiation has been suggested to be a viable emission process for GRBs (Katz, 1994, Tavani, 1996), there has since been much controversy over what radiation mechanism actually gives rise to the observed GRB spectra. Several studies (e.g., Ghissilini et al., 1999, Celotti & Ghissilini, 1999) have attempted to rule out synchrotron radiation as the source of GRB spectra based on certain discrepancies between the model’s predictions for the low energy spectral behavior and the observed data. In particular, the simple model of synchrotron radiation in an optically thin medium from a power law distribution of electrons with an isotropic pitch angle distribution (and neglecting radiation losses) predicts a value of the low energy photon index α of $-2/3$. The observed distribution of α is clearly inconsistent with this predicted behavior. The predicted value of α expected in a a simple cooling spectrum is $-3/2$, which is also inconsistent with the data. Furthermore it has been suggested (Crider et al., 1997) that the *variation* of α throughout the burst’s duration is inconsistent with what is expected from these synchrotron models.

In this paper, we show that synchrotron radiation can in fact explain the observed spectral behavior of GRBs. We show that the source of the discrepancies described above are a result of

two factors: a) the simplistic assumptions made in standard synchrotron models, b) assuming that the spectral fitting procedure accurately determines the asymptotic values of the spectral indices, without accounting for the effects of the detector bandwidth in the fitting procedure. [The latter effect must be accounted for not only when comparing to synchrotron models, but all other emission models as well.]

We focus on the so-called “instantaneous” synchrotron spectra (in which radiation losses are not evident). As mentioned above, the simple cooling spectrum is not consistent with observations. A cooling spectrum is obtained when electrons are injected in a magnetized region, where they then lose all of their energy to radiation; it is not clear that this is a viable scenario for GRBs. Although the “cooling time” (the timescale over which electrons lose their energy to radiation) is much shorter than other timescales involved in the fireball model (e.g. the hydrodynamical timescale), it is probably unrealistic to separate the acceleration and radiation loss processes at the site of the GRB. To sustain the burst, there should be continual acceleration of the emitting particles with a rate equal or greater than the synchrotron loss rate. In this case, particles can still lose all of their energy to radiation quickly, but we will have the instantaneous spectrum as a result of the competing acceleration and loss processes. [Note that because electrons are losing all of their energy to radiation, the efficiency (i.e. the ratio of energy radiated to the total energy of the GRB) in this model is the same as calculated using the simple cooling model - about 1% (see, e.g., Kumar, 1999).] We believe that this is an attainable scenario, although proof of this is beyond the aim of this paper.

To investigate whether the instantaneous synchrotron models are consistent with the existent data, we relax four important assumptions used in the usual analysis with synchrotron models: 1) We allow for the possibility of synchrotron self-absorption, which produces a hard low energy photon index of either 1 or $3/2$, depending on the relative values of the synchrotron self-absorption frequency and the minimum electron frequency. 2) We allow for a more realistic smooth (rather than sharp) cutoff to the electron distribution, which tends to soften the low energy spectral behavior. 3) We include effects of small pitch angle scattering, which leads to a value of α of 0. 4) We account for the fact that as the break energy of the GRB spectrum approaches the lower edge of the BATSE spectral window, the low energy spectral index will become softer (the expected asymptote of $-2/3$ is not reached). Items 1-3 above produce physically different low energy spectral behavior. Item 4 is a procedural and instrumental effect which leads to additional dispersion of the α distribution.

We show that including all of these effects can explain the observed distribution of α 's. We also infer from our analysis that the electron energy distribution must flatten or decline at low energies; otherwise, we would see many more bursts with $\alpha < -3/2$. GRBs whose α values lie above the “line of death” ($\alpha = -2/3$) may be explained either by emission from electrons with small pitch angles or absorption processes (e.g. synchrotron self absorption). Finally, we present some examples of the temporal behavior of GRB spectral parameters. We show that some of the temporal evolution is explained by the expected correlation between α and E_p , that results from the detector bandwidth and the fitting process. Other temporal variations in the spectral parameters suggest changes in the physical conditions at the GRB source from pulse to pulse

(where each pulse may represent independent emission episodes, for example, in an internal shocks model). A detailed study of the variety of spectral evolution and its consistency with synchrotron emission from internal shocks is the subject of an upcoming publication.

In this paper, we have dealt only with the low energy spectral index α . Similar discrepancies and limitations exist for the high energy spectral index β . However, the value of this index is not as well determined or reliable because the signal-to-noise decreases rapidly with energy, to an extent that it is questionable whether we even have a simple power law spectrum above E_p . However, there is some reliable data for bright bursts, and we shall explore the effects of modifications described here for β in a future publication.

Acknowledgements: This work was supported by the CGRO Guest Investigator Program and by the Stanford McMicking Fellowship. We would like to thank Rob Preece for many useful discussions, as well as providing and helping with the some of the BATSE data used in this analysis. We would also like to thank Pawan Kumar for helpful comments. Finally, we are greatly indebted to the referee for an extremely careful reading of the manuscript, and helpful comments which much improved this paper.

REFERENCES

- Band, D., et al. 1993, ApJ, 413, 281
- Brainerd, J.J. 1994, ApJ, 428, 21
- Celotti, A. & Ghissilini, G. 1999, in Gamma-Ray Bursts: The First Three Minutes, A.S.P. vol. 190, eds Juri Poutanen and Roland Svensson
- Crider, A., et al. 1997, ApJ, 479, L39
- Crider, A. & Liang, E.P. 1999, A&AS, 138, 405
- Dermer, C.D. & Boettcher, M. 2000, submitted to ApJL, astro-ph 0002306
- Dung, R. & Petrosian, V. 1994, ApJ, 421, 550
- Epstein, R.I. 1973, ApJ, 183, 593
- Epstein, R.I. & Petrosian, V. 1973, ApJ, 183, 611
- Ford, L.A., et al. 1995, ApJ, 439, 307
- Gallant, Y.A., et al. 2000, to appear in the proceedings of the 5th Huntsville Gamma Ray Burst Symposium; astro-ph 0001509
- Ghissilini, G. et al., 1999, to appear in MNRAS; astro-ph 9912461
- Granot, J. et al., 2000, submitted to ApJ; astro-ph 0001160
- Grusinov, A. & Mészáros, P. 2000, submitted to ApJL; astro-ph 0004336

- Guthman, A.W., et al. 2000, to appear in the proceedings of the 5th Huntsville Gamma Ray Burst Symposium; astro-ph 0002176
- Harris, M.J. & Share, G. H 1998, ApJ, 494, 724
- Katz, J.I. 1994, ApJ, 432, L107
- Kirk, J.G. et al., 2000, submitted to ApJ; astro-ph 0005222
- Kumar, P. 1999, ApJ, 523, L113
- Liang, E.P. & Kargatis, V.E. 1996, Nature, 381, 49
- Lloyd, N.M. & Petrosian, V. 1999, ApJ, 511, 550
- Lyutikov, M. & Blackman, E.G. 2000, astro-ph 0004212
- Medvedev, M.V. 2000, submitted to ApJ; astro-ph 0001314
- Norris, J.P., et al. 1986, ApJ, 301, 213
- Pacholczyk, A.G. 1970, Radio Astrophysics (W.H. Freeman and Company: San Francisco)
- Papathanassiou, H. 1998, A&AS, 138, 525
- Park, B. & Petrosian, V. 1995, ApJ, 446, 699
- Petrosian, V. & Donaghy, T.Q. 1999, ApJ, 527, 945
- Piran, T. 1999, Physics Reports, 314, 575
- Preece, R.D., et al. 1998a, ApJ, 506, L23
- Preece, R.D., et al. 1998b, ApJ, 496, 849
- Preece, R.D., et al. 1999, ApJS, 126, 19
- Pryadko, J. & Petrosian, V. 1998, ApJ, 495, 377
- Sari, R., Piran, T., & Narayan, R. 1998, ApJ, 497, L17
- Strohmeyer, T.E., et al. 1998, ApJ, 500, 873
- Tavani, M. 1996, ApJ, 466, 768